JOURNAL OF MATERIALS SCIENCE 21 (1986) 4359–4365

The cubic-to-β martensitic transformation in ZrO_2–Sc_2O_3

T. SAKUMA, H. SUTO
Department of Materials Science, Faculty of Engineering, Tohoku University, Sendai 980, Japan

The nature of the cubic-to-β (c–β) transformation and the microstructure of the β-phase were examined in ZrO_2–10.5 and 12.5 mol % Sc_2O_3 alloys. The c–β transformation is induced during cooling from the high-temperature cubic phase region by martensitic transformation. The microstructure of the β-phase usually has a herring-bone appearance, which is made of a unique array of four orientation variants. Two types of interfaces are formed in the structure; long straight interfaces and short interfaces. The former and the latter interfaces are nearly parallel to the $\{0\,1\,1\}_\beta$ and $\{1\,1\,2\}_\beta$ type planes, respectively, which correspond to the $\{0\,0\,1\}_c$ and $\{0\,1\,1\}_c$ planes in the parent cubic phase. The $\{0\,1\,1\}_\beta$ and $\{1\,1\,2\}_\beta$ type interfaces are fully coherent, low-energy interfaces. The herring-bone structure is likely to be a favourable one for minimizing the strain energy and interfacial energy associated with the c–β transformation, which is a characteristic microstructure developed by martensitic transformation.

1. Introduction

The scandia-stabilized zirconia (SSZ) containing 6 to 12 mol % Sc_2O_3 has an excellent ionic conductivity at high temperatures [1]. The conductivity of SSZ is the highest among zirconia ceramics at 1000° C [1], but decreases rapidly with temperature below about 800° C. Annealing at 800° C for 200 h causes a 40 to 50% decrease in ionic conductivity in SSZ with 8 to 9 mol % Sc_2O_3 [2, 3]. The decrease in conductivity below 800° C is one of the reasons why SSZ is not practically used for devices. Such a decrease is believed to be due to the formation of the β-phase during annealing [2]. However, the generation of the β-phase at 800° C is not expected from the ZrO_2–Sc_2O_3 phase diagram [1, 4]. Uncertainty remains in the reported phase diagram and the nature of the cubic-to-β(c–β) transformation. This is partly related to the complexity of the ZrO_2–Sc_2O_3 system. The system has three intermediate phases, β, γ and δ which are non-stoichiometric phases with a relatively wide composition range. The three phases have a rhombohedral distortion from the parent fluorite structure. It has been clarified that the distortion in the γ and δ phases is caused by lattice relaxation due to ordered omission of oxygen ions from the fluorite structure [5]. In addition to the study of the crystal structure of parent and product phases, microstructural observations are also useful in understanding the transformation characteristics, which are substantially related to ionic conductivity.

In the present study, the microstructure of the β-phase was examined in detail to elucidate the nature of the c–β transformation.

2. Experimental procedure

The materials used were zirconia and scandia powders with 99.9% purity supplied by Rare Metallic Co Ltd (Tokyo) and Japan Yttrium Co Ltd (Mitaka City, Tokyo), respectively. They were mixed in a ball mill and then pelleted in a steel die. The pellets were sintered at 1400° C and then arc-melted in an argon atmosphere. After arc-melting, the samples were cooled on a water-cooled copper hearth. They were button-shaped and had a weight of about 1 g. The cooling rate after melting was about the same with that reported in a previous paper [6]. The composition of alloys was ZrO_2–10.5 mol % Sc_2O_3 (alloy 1) and ZrO_2–12.5 mol % Sc_2O_3 (alloy 2). The local compositional change was less than 10% of the average composition of each alloy. Arc-melted alloys are termed as-cast alloys in the text. Some of the as-cast alloys were annealed at 1000° C for 24 h in air, and then water-quenched (quenched alloy) or furnace-cooled (furnace-cooled alloy). Phosphoric acid at 230° C was used as an etchant for revealing the microstructure. Thin foils for electron microscopy were prepared, using an ion-beam milling apparatus, from the polished discs with 3 mm diameter and ~0.1 mm thickness. They were examined in a JEM 200B electron microscope operated at 200 kV. Samples for X-ray diffraction (XRD) analysis were prepared by crushing the alloys in a mortar. Room- and high-temperature X-ray analyses were made by Shimazu (Kyoto) VD-1 and Rigaku (Tokyo) RU 200PL X-ray diffractometer, respectively.

3. Results

3.1. X-ray diffraction

Fig. 1 shows the X-ray intensity profiles of the two as-cast alloys at room temperature. The $1\,1\,1_c$, $2\,2\,0_c$, and $3\,1\,1_c$ reflections in the cubic fluorite structure are separated into two or three peaks in the two alloys. The separation is characteristic of the rhombohedral

0022–2461/86 $03.00 + .12

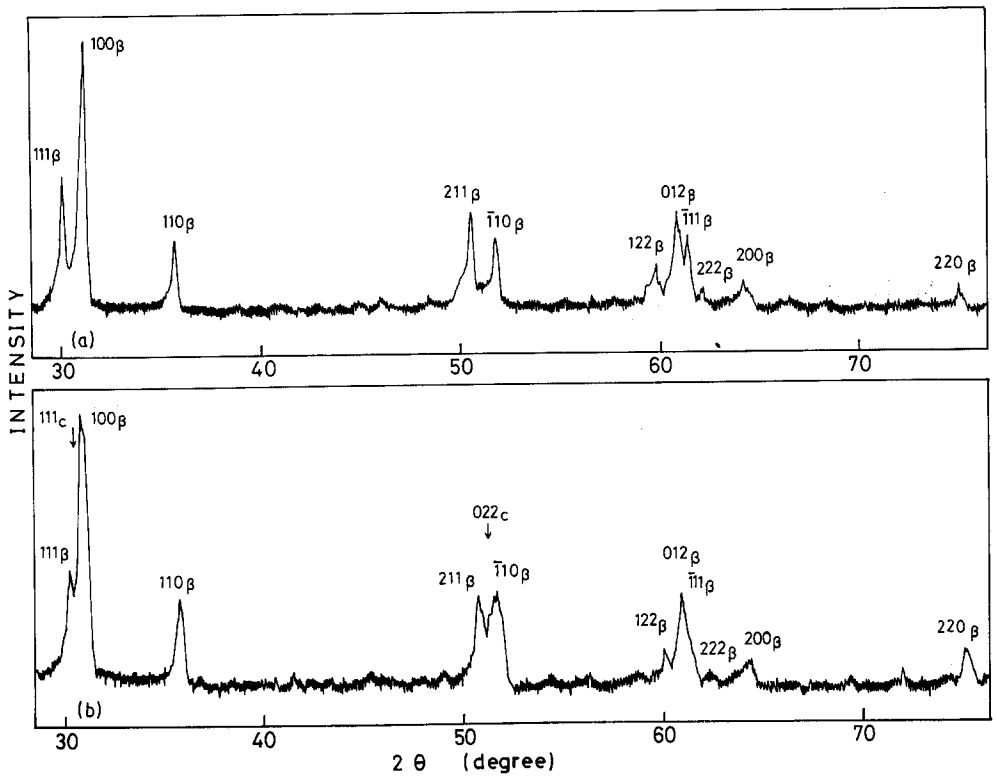

Figure 1 Room-temperature X-ray diffraction patterns for (a) ZrO_2–10.5 mol % Sc_2O_3, (b) ZrO_2–12.5 mol % Sc_2O_3.

β-phase. The location of peaks from the β-phase is well explained by the reported lattice parameter $a' = 0.5085$ nm ($a = 0.3633$ nm) and the rhombohedral angle $\alpha' = 88.8°$ ($\alpha = 58.6°$) [7]. The separations of $1\,1\,1_\beta$ from $1\,0\,0_\beta$, and also of $2\,1\,1_\beta$ from $1\,1\,0_\beta$ are clear in alloy 1 but not in alloy 2. It is likely that $1\,1\,1_c$ and $0\,2\,2_c$ peaks appear, i.e. the c-phase is partly retained in alloy 2. The result was confirmed by electron microscopy described later.

Fig. 2 shows the high-temperature X-ray diffraction data in alloy 1, which was obtained during cooling from 1000° C. The single $1\,1\,1_c$ peak is obtained at 1000° C, but two peaks, $1\,1\,1_\beta$ and $1\,0\,0_\beta$, appear below 800° C. The alloy is composed of c-phase at 1000° C, while the β-phase is present below 800° C. A similar result was obtained in alloy 2. The result indicates that the c-phase is not stable below about 800° C in SSZ with 10.5 and 12.5 mol % Sc_2O_3. The present data seem to support that the marked decrease in ionic conductivity at 800° C is caused by generation of the β-phase, as expected previously [3].

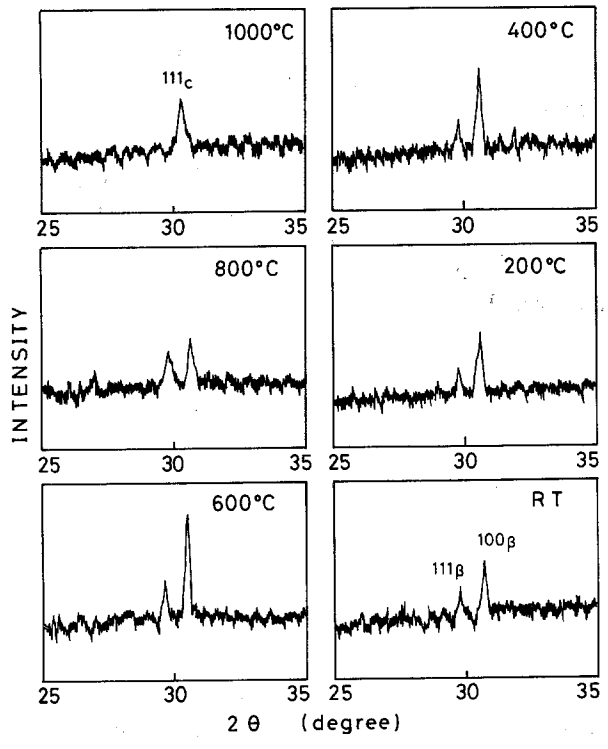

Figure 2 High-temperature X-ray diffraction patterns in alloy 1.

3.2. Optical microscopy

Fig. 3 shows the optical micrographs of as-cast alloys. In the two alloys, a white lenticular phase is embedded in the phase with a striped pattern. It was confirmed by electron microscopy that the former is c-phase retained at room temperature and the latter is the β-phase. Fig. 3 shows that the c-phase is partly retained in both alloys at room temperature. On the other hand, the presence of retained c-phase is verified by XRD only in as-cast alloy 2, but not in alloy 1 (Fig. 1). The disagreement between optical microscopy and XRD data in alloy 1 could be caused by the fact that the samples for XRD were prepared by crushing as-cast alloys in a mortar. It has been reported that phase transformation is sometimes induced by crushing or mechanical polishing in Y–PSZ [6, 8]. The c-phase retained in alloy 1 in the as-cast state is likely to be transformed to the β-phase during crushing. Fig. 1b shows that the c-phase is still present in crushed powders in alloy 2. The c-phase with higher scandia content must be more stable than that with a lower content, because scandia is a cubic-stabilizing oxide.

Fig. 4 shows the optical micrograph of quenched

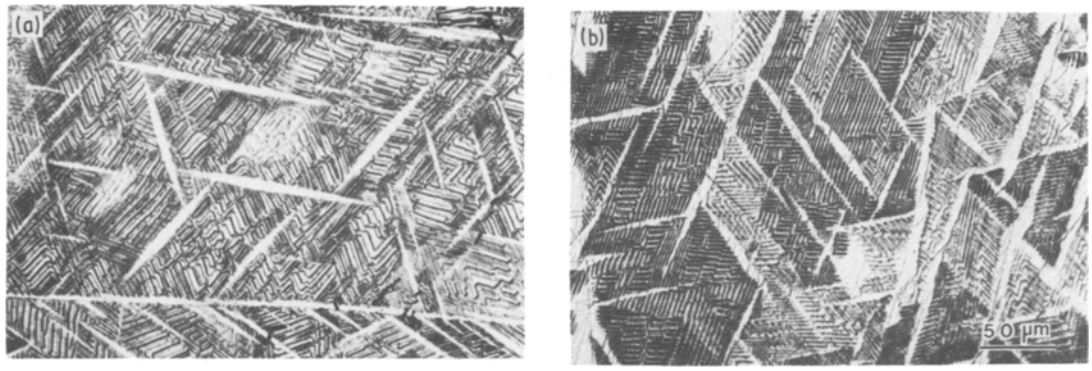

Figure 3 Optical micrographs of as-cast alloys: (a) alloy 1; (b) alloy 2.

alloy 1. It was found that the c-phase was not retained in the quenched or furnace-cooled alloy. The c-phase disappeared upon heat treatment in both alloys. Some cracks are introduced along grain boundaries in prior c-phase (Fig. 4). The microstructure of the β-phase consists of several packets with different orientations in a prior c-phase grain.

Fig. 5 shows the structure of the β-phase in the quenched alloy taken in a higher magnification. The principal microstructure of the β-phase is the so-called "herring-bone" appearance [3, 4], which has straight interfaces as found in the lower part in Fig. 5. In the upper left part of Fig. 5, the β-phase with wavy interfaces is seen. The wavy interfaces were more often found in the quenched alloy than the furnace-cooled alloy. Well-developed herring-bone structure was commonly observed in the furnace-cooled alloy. An example of the structure in alloy 1 is shown in Fig. 6.

3.3. Electron microscopy

Fig. 7 shows the electron micrograph in the as-cast alloy 1. The herring-bone structure is seen in the figure, which is made of lamellae with long straight interfaces. The straight interface, such as A in Fig. 7, has a fringe contrast showing that the interface is inclined to the electron beam direction. The straight interface is termed primary interface in this paper. Each lamella consists of many blocks divided by short straight interfaces such as B in Fig. 7, which we term secondary interfaces. The contrast of blocks changes alternately. This is due to the fact that each block is composed of a particular variant of the β-phase and alternate blocks have the same orientation variant, as shown later. The c-phase is retained in a central part shown by an arrow, C in Fig. 7.

Fig. 8 shows the boundary between c- and β-phases in as-cast alloy 2. The diffraction pattern, Fig. 8b, was taken from the encircled region in Fig. 8a, which was indexed by cubic fluorite structure. Dislocations are emitted in the c-phase near the boundary. It has been reported that dislocations are often induced in cubic zirconia at high temperatures [6]. The dislocations in Fig. 8 are probably induced for relieving the strain associated with the c–β transformation.

Fig. 9 shows the β-phase with wavy interfaces in the as-cast alloy 2. The contrast of the wavy interfaces is very complicated. It is not clear at present why the wavy interfaces sometime develop in the β-phase.

Fig. 10 shows part of the herring-bone structure in the as-cast alloy 2. The diffraction pattern was taken from the encircled region in Fig. 10a. The beam direction is close to $[0\,1\,\bar{1}]_\beta$. The patterns from two variants appear in Fig. 10b. It is noted that the $0\,1\,1_\beta$ reflections from the two variants are overlapped but the $2\,1\,1_\beta$ reflections are split. The primary interface runs nearly parallel to the electron beam direction in Fig. 10a, which is close to the $(0\,1\,1)_\beta$ plane. The habit planes in the herring-bone structure were also determined by conventional trace analysis. The result shows that the primary interface is also close to the $\{0\,1\,1\}_\beta$ type planes. The distortion axes $[1\,1\,1]_\beta$ of the two variants in Fig. 10a are in the photographic plane. The angle between $2\,1\,1_\beta$ from the two blocks was estimated to be 3.5°, which agrees well with the calculated angle 3.4° from the reported lattice parameter and rhombohedral angle [7].

Fig. 11 is the structure of as-cast alloy 2 taken from the beam direction close to $[1\,1\,\bar{1}]_\beta$. The primary and secondary interfaces run nearly parallel to the beam direction in Fig. 11. The diffraction pattern in

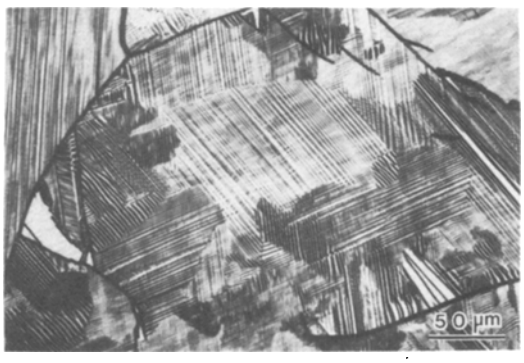

Figure 4 Structure of quenched alloy 1.

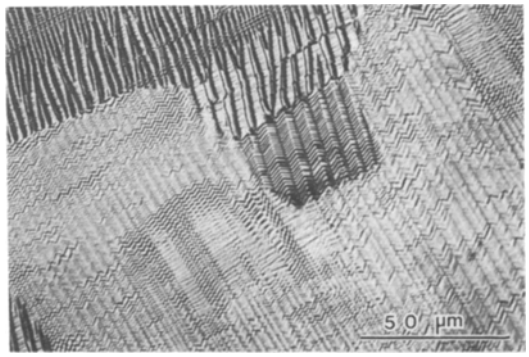

Figure 5 Optical micrograph of the β-phase in quenched alloy 2. The β-phase with different morphologies is formed.

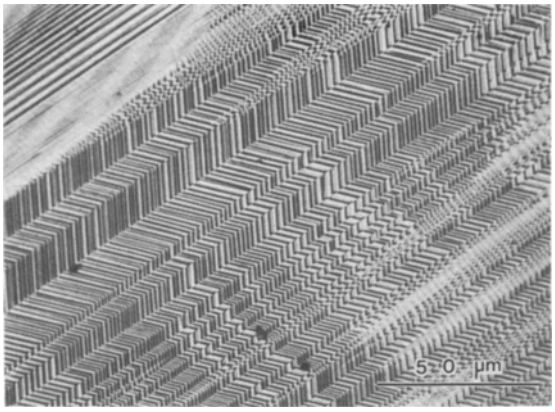

Figure 6 Well-developed herring-bone structure in furnace-cooled alloy 1.

Fig. 11b was taken from block 1. The angle between $0\,\bar{1}\,\bar{1}_\beta$ and $1\,0\,1_\beta$ is about 91°. In combination with diffraction patterns such as Figs 10b and 11b, the distortion axis $[1\,1\,1]_\beta$ in a block is uniquely decided. The result is shown by bars in Fig. 11a, which indicate the traces of $[1\,1\,1]_\beta$ in each variant. The traces are parallel between blocks 1 and 2, and also between 5 and 6 on the photographic plane. However, they are inclined to each other and the respective two blocks are different in orientation. The rhombohedral structure of the β-phase is obtained by a distortion of fluorite structure in the $[1\,1\,1]_\beta$ direction. There are four orientation variants in the β-phase, because four equivalent $\langle 1\,1\,1\rangle_c$ directions exist in the parent c-phase. Fig. 11 shows that the herring-bone structure is made of alternate array of the four orientation variants. The primary and secondary interfaces are known to be close to the $(0\,1\,1)_\beta$ and $(1\,1\,2)_\beta$ planes in Fig. 11. The habit plane of the secondary interfaces was also confirmed by trace analysis. It should be pointed out that there are three equivalent $\{0\,1\,1\}_\beta$ and $\{1\,1\,2\}_\beta$ planes in the rhombohedral β-phase. The habit planes with different $\{0\,1\,1\}_\beta$ or $\{1\,1\,2\}_\beta$ type planes are seen in Fig. 7. For example, the direction of the long straight interfaces in the upper part is different from the lower part in Fig. 7. This is due to the fact that the two different $\{0\,1\,1\}_\beta$ type planes become habit planes in this area. The microstructure of the β-phase is composed of many packets as seen in Figs 4 and 7. Each packet has the primary interface close to one of the $\{0\,1\,1\}_\beta$ type planes. It is possible for all the equivalent $\{0\,1\,1\}_\beta$ and $\{1\,1\,2\}_\beta$ type planes to become habit planes.

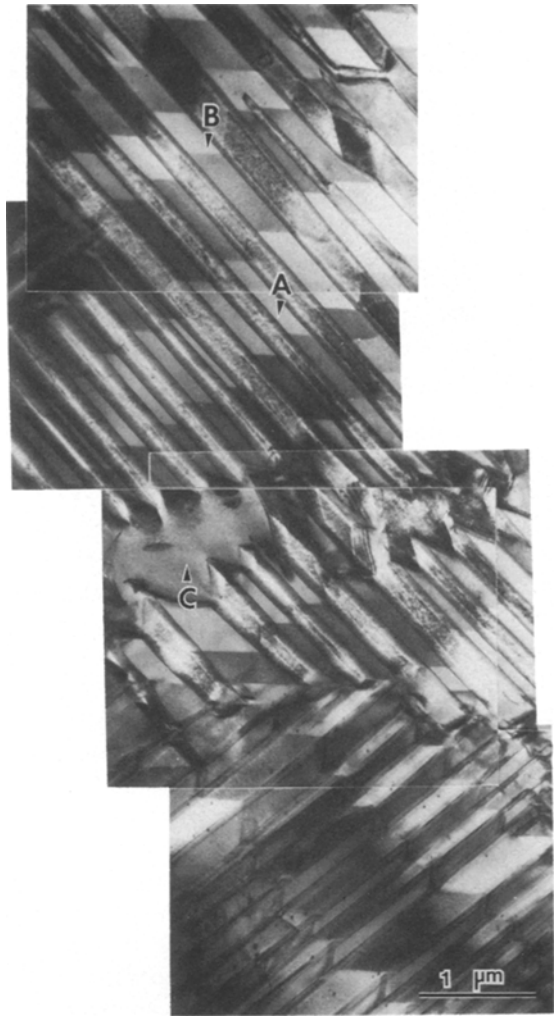

Figure 7 The microstructure of as-cast alloy 1. The β-phase has a herring-bone appearance, while the c-phase is retained in a central part marked C in the photograph.

It was found that small dislocation loops were formed in quenched and furnace-cooled alloys. An example is shown in Fig. 12 in quenched alloy 2. Dislocation loops in the herring-bone structure are probably introduced during heating at 1000° C, because the loops are more often observed in the quenched or furnace-cooled alloy rather than in the as-cast alloy. Extrinsic oxygen vacancies are introduced by an addition of Sc_2O_3 to ZrO_2. Judging from the extrinsic vacancy concentration, the loop density in Fig. 12 is very low, i.e. only a small part of vacancies cluster into loops during annealing. Oxygen vacancies tend to order in the β-phase, which results in

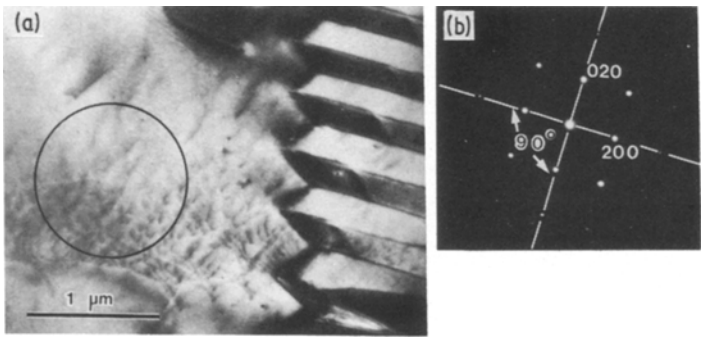

Figure 8 Electron micrograph of as-cast alloy 2 showing the structure in the vicinity of the c/β boundary (a). The diffraction pattern (b) was taken from the encircled region in (a).

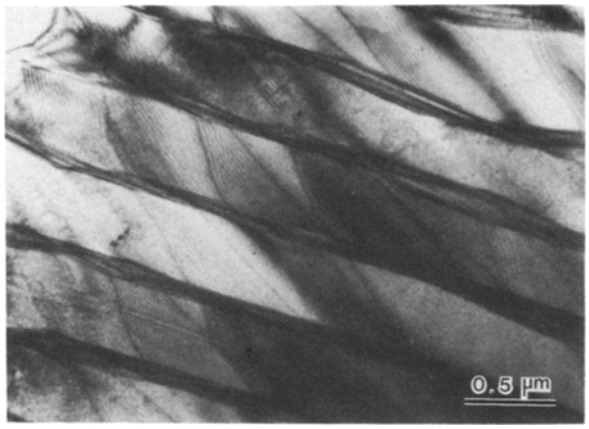

Figure 9 The β-phase with wavy interfaces in as-cast alloy 2.

extra reflections in the diffraction pattern. Fig. 13 shows an example of the electron diffraction patterns accompanying the extra reflections caused by oxygen ordering. The extra reflections have a three-fold symmetry on the photographic plane, as well as principal reflections, which are generated from cations in the rhombohedral lattice. The array of extra reflections is slightly rotated with principal reflections about the $[1\,1\,1]_\beta$ axis, which is parallel to the electron beam direction. The ordering of oxygen vacancies expected from the array of extra reflections resembles that in the γ and δ phases [5]. However, the spacing between rows of vacancy ordering estimated from the distance between the extra reflections in Fig. 13 was about twice as large as that in the γ and δ phases. This is probably due to the low concentration of extrinsic vacancies in the β-phase in comparison with the γ and δ phases. Further detailed analysis on oxygen ordering could not be made from the diffraction pattern such as Fig. 13, which includes the patterns from two different orientation variants. Microdiffraction or lattice imaging by electron microscopy is required for more precise analysis of vacancy ordering.

4. Discussion

4.1. Phase diagram in ZrO_2–Sc_2O_3 system

The ZrO_2–Sc_2O_3 phase diagram was determined by Spiridonov *et al.* [1] and Ruh *et al.* [4]. There is some disagreement between the two reported diagrams. In the region where the β-phase is concerned, the single β-phase region is narrow around ideal stoichiometry $Zr_7Sc_2O_{17}$ in the former diagram, while a wider region is shown in the latter. The present data show that the β-phase is a principal phase below about 800° C in the two alloys, with a scandia content of 10.5 and 12.5 mol %. It seems that the β-phase region is a little wider than that reported by Spiridonov *et al.* [1] and is rather close to that shown by Ruh *et al.* [4]. However, the β-phase appears at higher temperatures than shown in the two reported diagrams. Uncertainty still remains in the vicinity of the β-phase region in ZrO_2–Sc_2O_3 system, which is probably related to the difficultly of attaining the equilibrium around 800° C.

4.2. Herring-bone structure of the β-phase

The present observation has revealed that the β-phase usually has a unique microstructure with a herring-bone appearance. The herring-bone structure is made of alternate array of four orientation variants in the β-phase (Fig. 11). The habit planes of primary and secondary interfaces are close to the $\{0\,1\,1\}_\beta$ and $\{1\,1\,2\}_\beta$ type planes, respectively. Fig. 14 shows an array of ions near the $(0\,1\,1)_\beta$ and $(1\,1\,2)_\beta$ interfaces on the $(1\,1\,0)_\beta$ plane. The $(0\,1\,1)_\beta$ and $(1\,1\,2)_\beta$ habit planes make angles of 91.2° and 91.7°, respectively, with the $(1\,1\,0)_\beta$ plane. In the figure, open circles represent oxygen ions on the plane of the paper, while filled and striped circles represent cations which are $a'/4$ above and below the plane, respectively. The crystal structure of the β-phase is described by the stacking of the three successive layers of ions. The same figure can be drawn on all the equivalent $\{0\,1\,1\}_\beta$ type planes. Fig. 14 shows that the herring-bone structure is constructed by a special array of ions, and that the $(0\,1\,1)_\beta$ and $(1\,1\,2)_\beta$ interfaces are coherent. The situation is the same when other $\{0\,1\,1\}_\beta$ or $\{1\,1\,2\}_\beta$ type planes become habit planes. It may be necessary to point out that the actual interfaces in the β-phase are not always and not so strictly parallel to the $\{0\,1\,1\}_\beta$ or $\{1\,1\,2\}_\beta$ type planes. For example, the interface is sometimes slightly curved (arrow in Fig. 10) and adjacent straight interfaces are not parallel to each other (Fig. 12). Generally speaking, however, the interfaces in the herring-bone structure are nearly parallel to the $\{0\,1\,1\}_\beta$ or $\{1\,1\,2\}_\beta$ type planes. It has been accepted that coherent interfaces such as $(0\,1\,1)_\beta$ and $(1\,1\,2)_\beta$ are low-energy interfaces in solids [9]. It seems that low-energy interfaces tend to be formed in the β-phase.

It is noted that two crystals bounded by a primary or secondary interface have a special orientation relationship. The two crystals are rotated with respect to each other by π about the direction $[1\,0\,0]_\beta$ in the $(0\,1\,1)_\beta$ interface. It is also possible to match one crystal with another on the $(1\,1\,2)_\beta$ interface by a rotation of π about the interface plane normal. The $[1\,0\,0]_\beta$ direction

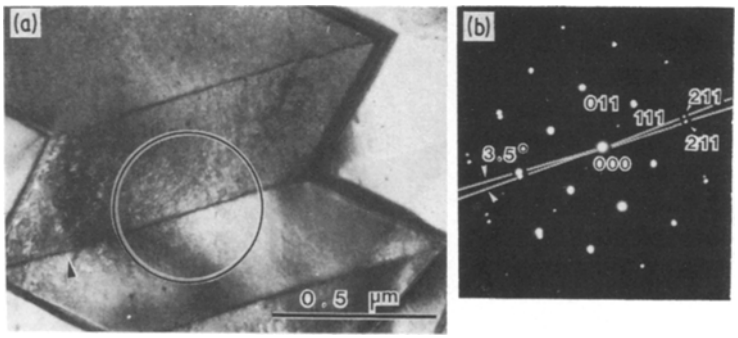

Figure 10 Electron micrograph of the β-phase in as-cast alloy 2. The diffraction pattern taken from the encircled region in (a) is shown in (b).

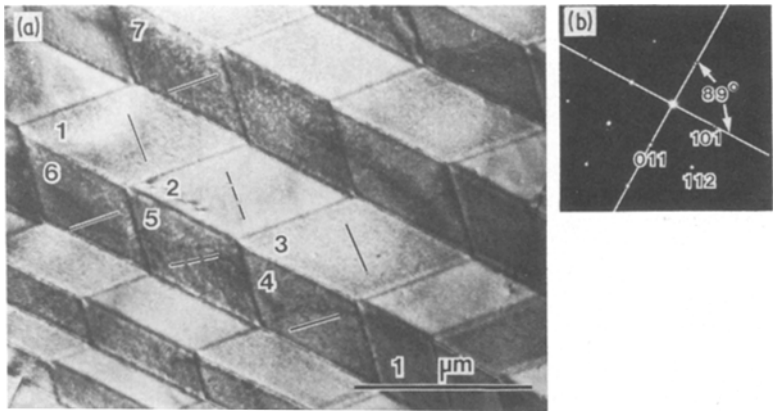

Figure 11 The microstructure of the β-phase taken from the beam direction close to $[1\,1\,\bar{1}]_\beta$. The bars in (a) are the traces of $[1\,1\,1]_\beta$ in each block. The diffraction pattern (b) is that taken from a single block 1 in (a).

corresponds to $[1\,1\,0]_c$, which is the shear direction in the parent c-phase [10]. The crystals bounded by the interfaces have a similar crystallographic relationship with deformation twins [11].

4.3. Nature of the c–β transformation

The present study has revealed that the β-phase is produced in alloys quenched from the cubic-phase region (Figs 4, 5 and 12). The diffusion of constituent ions would be suppressed by the quenching. The result suggests that the c–β transformation is martensitic in nature. The structural features of the β-phase have some similarities to those formed by martensitic transformation in ceramics and metallic alloys. First of all, several packets of the β-phase with different orientation are formed in a prior c-phase as seen in Fig. 4, which resembles the α' martensite in a prior austenite grain in steels [12]. Secondly, it has been reported in ZrO_2–Y_2O_3 [6, 13] and Au–Cd alloys [14] that the herring-bone structure is developed by martensitic transformation. It is likely that the herring-bone structure is effective for minimizing the strain energy associated with the c–β transformation [3]. The minimization is essentially important in diffusionless transformation, because a considerable part of the driving force for the transformation is consumed by the strain energy [15]. Thirdly, dislocations are emitted in the c-phase at the transformation front (Fig. 8). Dislocations or twins are often induced to accommodate the strain in martensitic transformation [15]. Fourthly, the interfaces in the herring-bone structure are mainly composed of low-energy, coherent interfaces as mentioned in the previous section. The development of low-energy interfaces is also favourable for martensitic transformation [15]. It is, therefore, reasonable to conclude that the c–β transformation in ZrO_2–Sc_2O_3 occurs by martensitic transformation.

5. Conclusion

The c–β transformation was examined in the two ZrO_2–Sc_2O_3 alloys with scandia contents of 10.5 and 12.5 mol %. The results obtained are:

1. The β-phase was produced during cooling from high-temperature cubic phase region. The c–β transformation was induced both in the quenched and furnace-cooled alloys;
2. The principal microstructure of the β-phase is that with a unique herring-bone appearance. The structure is constructed by an alternate array of the four orientation variants of the β-phase. The interfaces between variant crystals are straight and mainly consist of either $\{0\,1\,1\}_\beta$ or $\{1\,1\,2\}_\beta$ type planes, which

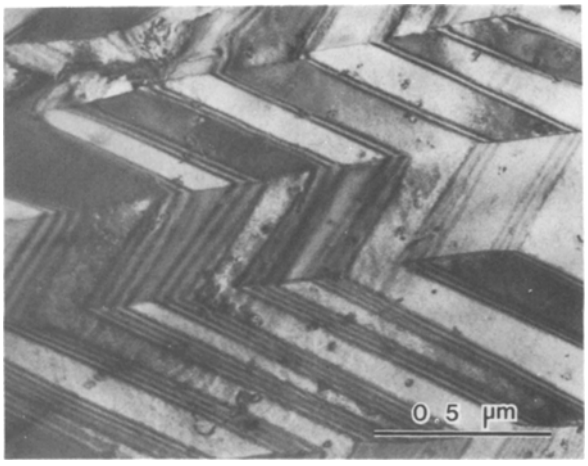

Figure 12 The microstructure of quenched alloy 2. Dislocations and loops are seen.

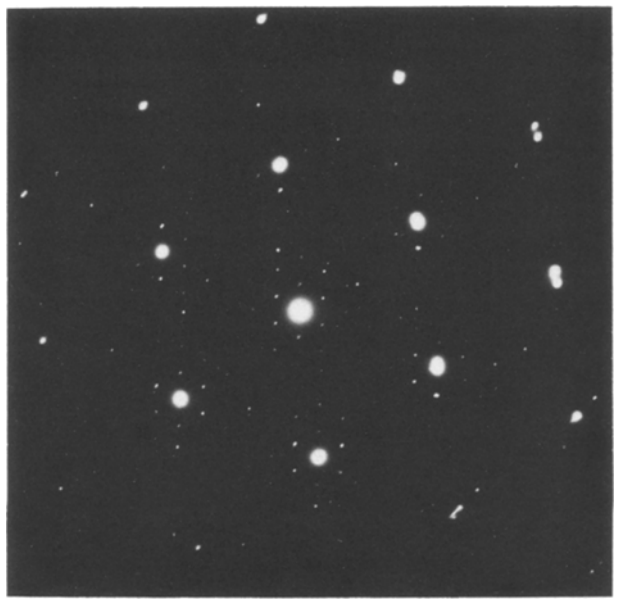

Figure 13 Diffraction patterns taken from the beam direction close to $[1\,1\,1]_\beta$. The principal reflections are originated from cations in the rhombohedral lattice of the β-phase and weak reflections are generated by ordering of oxygen ions.

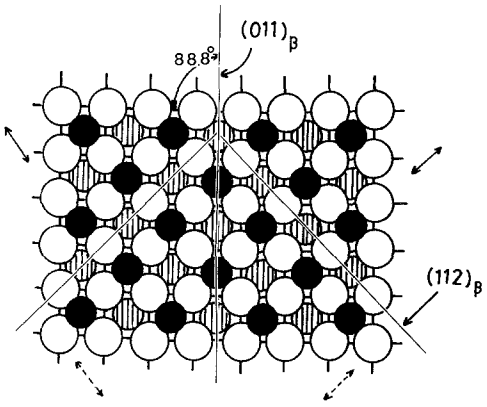

Figure 14 Array of ions in herring-bone structure. Stacking of ions on the $(1\,1\,0)_\beta$ plane is shown. The arrows show the traces of distortion axis $[1\,1\,1]_\beta$.

are fully coherent. The former appears as long and straight interfaces, but the latter is short one;

3. The β-phase with curved interfaces was sometimes produced. The curved interfaces were more often found in the quenched alloy than in the furnace-cooled alloy;

4. The c–β transformation is martensitic in nature, because the transformation is induced by water quenching. The microstructure of the β-phase has characteristic features of martensite.

Acknowledgements

The authors wish to thank Mr Ohkubo for his experimental assistance. The present work was supported by a Grant-in-Aid Ippan B-60470063 for Fundamental Scientific Research 1985–1986 from the Ministry of Education, Japan.

References

1. F. M. SPIRIDONOV, L. N. POPOVA and R. YA. POPIL'SKII, *J. Solid State Chem.* **2** (1970) 430.
2. M. V. INOZEMTSEV, M. V. PERFILEV and V. P. GORELOV, *Sov. Electrochem.* **12** (1976) 1128.
3. F. K. MOGHADAM, T. YAMASHITA, R. SINCLAIR and D. A. STEVENSON, *J. Amer. Ceram. Soc.* **66** (1983) 213.
4. R. RUH, H. J. GARRETT, R. F. DOMAGALA and V. A. PATEL, *ibid.* **60** (1977) 399.
5. M. R. THORNVER and D. J. M. BEVAN, *Acta Crystallogr.* **B24** (1968) 1183.
6. T. SAKUMA, Y. YOSHIZAWA and H. SUTO, *J. Mater. Sci.* **20** (1985) 2399.
7. J. LEFEVRE, *Ann. Chim.* **8** (1963) 117.
8. H. HASEGAWA, *J. Mater. Sci. Lett.* **2** (1983) 91.
9. C. LAIRD and R. SANKARAN, *J. Microscopy* **116** (1979) 123.
10. A. G. EVANS and P. L. PRATT, *Phil. Mag.* **20** (1969) 1213.
11. J. P. HIRTH and J. LOTHE, "Theory of dislocations" (McGraw-Hill, New York, 1968) p. 738.
12. J. M. MARDER and A. R. MARDER, *Trans. Amer. Soc. Metals* **62** (1969) 1.
13. T. SAKUMA, Y. YOSHIZAWA and H. SUTO, *J. Mater. Sci. Lett.* **4** (1985) 29.
14. T. TADAKI, Y. KATANO and K. SHIMIZU, *Acta Metall.* **26** (1978) 883.
15. J. W. CHRISTIAN, "The mechanism of phase transformations in crystalline solids"Monograph and Report Series No. 33 (The Institute of Metals, London, 1969) p. 129.
16. E. C. SUBBARAO, H. S. MAITI and K. K. SRIVASTAVA, *Phys. Status Solidi* (*a*) **21** (1974) 9.

Received 21 January
and accepted 14 March 1986